

Pull-In Instability and Vibrations of a Beam Micro-Gyroscope

Mahdi Moghimi Zand^{1*}, Amir Ostadi Moghaddam²

1. Assistant Professor, School of Mechanical Engineering, University of Tehran, Tehran, Iran

2. Department of Mechanical Engineering, University of Tehran, Tehran, Iran

Received 18 July 2014; Accepted 7 October 2014

Abstract

Gyroscopes are used as rotation rate sensors. Conventional gyroscopes are heavy and bulky, which creates important problems regarding their usage in different applications. Micro-gyroscopes have solved these problems due to their small size. The beam micro-gyroscope is one of the popular types of inertial sensors. Their small dimensions and low energy consumption are key reasons for their popularity. In this investigation, the model of an electrostatically actuated beam-based micro-gyroscope is used to study the effect of design parameters on pull-in voltage and fundamental frequency. The micro-gyroscope includes a rotating cantilever beam and a tip mass attached to the free end. DC voltages are applied to both sense and drive electrodes to actuate the system. The tip mass is actuated by an AC voltage in the drive direction to produce oscillations in the sense direction. Equations of motion are solved numerically to study different pull-in and vibrational parameters. Eigenvalues of the uncoupled system are computed to obtain the fundamental frequency of the micro beam for different values of DC voltages and design parameters. The frequencies are computed and validated with those in the literature. The results are beneficial for the design process of micro-gyroscopes.

Keywords: *beam micro-gyroscope, design parameters, natural frequency, pull-in voltage.*

1. Introduction

Position and orientation sensors have become an integral part of many modern engineering systems such as satellites, vehicles, and robots. Continuous progress in micromachining has significantly increased the accuracy and reliability of Micro-Electro-Mechanical System (MEMS) inertial sensors and played a crucial role in revolutionizing the related

industries. MEMS sensors have been studied in many research papers [1-10].

Gyroscopes are widely used as rotation rate sensors. Conventional gyroscopes are heavy, costly, and bulky, which imposes major limitations their use in demanding applications. Micro-gyroscopes have solved the abovementioned problems to a large degree and have become the object of intensive study in order to satisfy new market demands.

Although an enormous variety of gyroscopes with different features exist, the basic operation

* Corresponding Author. Tel.: +989133108601
Email Address: mahdimoghimi@ut.ac.ir

principle of their architecture is to generate and maintain a constant linear or angular momentum coupled to the sense mode. In the linear vibration gyroscope, a proof mass oscillates in the drive direction by an altering force. When the frame rotates, the Coriolis force generates oscillations orthogonal to the drive direction. The angular velocity can be estimated by measuring the amplitude of oscillations.

The beam micro-gyroscope is one of the most widely used types of inertial sensors. Batch production, small size and low energy consumption are some of the reasons for its popularity. Shupe and Connor first introduced the beam micro-gyroscope in 1983 [11]. They used an electrostatic force with a frequency near the fundamental frequency of a cantilever beam as excitation and a piezoelectric element for sensing the induced vibrations.

Maenaka et al. used piezoelectric actuators to excite a tip mass in the drive direction [12]. Capacitance variation between proof mass and sense electrode was used to identify the induced sense oscillations. Seok and Scarton derived a mathematical model for a cantilever beam excited by a distributed electrostatic force and investigated the eigenvalues of the system [13]. Esmaili et al. introduced an elementary model of a beam mass gyroscope considering an Euler-Bernoulli beam excited by electrostatic force [14]. They obtained a solution for the frequency equation and investigated the effect of excitation amplitude at the resonance frequency on the gyroscope output to input rotations.

Ghommen and Nayfeh developed a mathematical model of a beam micro-gyroscope excited by a pair of DC and AC voltages and obtained closed-form solutions for the linearized problem [15]. They investigated the relationship between the base rotation and gyroscopic coupling.

In the current research, we investigate the variation of pull-in voltage and first natural frequency of the micro beam with the input DC voltage for different values of design parameters. Results can be used as a guideline for selecting appropriate design values.

2. Equations of motion

A tip mass M is attached to the free end of a cantilever beam and oscillates in two

orthogonal directions. Equal DC voltages are applied in both directions to constrain the motion to flexural displacements and an AC voltage as an excitation to connect the orthogonal vibrations via angular velocity. We assume that the beam has a square uniform cross-section.

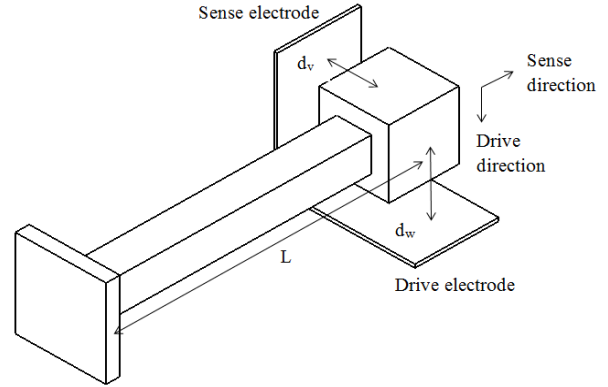


Fig. 1. Schematic of the cantilever beam with tip mass

Following Nayfeh et al. the equations of motion are obtained as follows [15]:

$$EIv^{(4)} - mv\Omega^2 + 2Jv''\Omega^2 - 2m\dot{w}\Omega + m\ddot{v} - mw\dot{\Omega} - \dot{\Omega}Jw'' - J\ddot{v} = 0 \quad (1)$$

$$EIw^{(4)} - mw\Omega^2 + 2Jw''\Omega^2 + 2m\dot{v}\Omega + m\ddot{w} + mv\dot{\Omega} - \dot{\Omega}Jv'' - J\ddot{w} = 0 \quad (2)$$

The associated boundary conditions at $x=0$:

$$v = w = 0 \quad (3)$$

$$v' = w' = 0 \quad (4)$$

and at $x=L$:

$$EIv''' + Mv\Omega^2 + 2Jv'\Omega^2 + 2M\dot{w}\Omega - M\ddot{v} + Mw\dot{\Omega} - \dot{\Omega}Jw' - J\ddot{v}' = -\frac{\varepsilon A_v V_{DC}^2}{2(d_v - v)^2} \quad (5)$$

$$EIw''' + Mw\Omega^2 + 2Jw'\Omega^2 - 2M\dot{v}\Omega - M\ddot{w} - Mv\dot{\Omega} - \dot{\Omega}Jv' - J\ddot{w}' = -\frac{\varepsilon A_w (V_{DC} + V_{AC})^2}{2(d_w - w)^2} \quad (6)$$

$$v'' = w'' = 0 \quad (7)$$

Introducing the following non-dimensional parameters:

$$\hat{x} = \frac{x}{L}, \quad \hat{v} = \frac{v}{d_v}, \quad \hat{w} = \frac{w}{d_w}, \quad \hat{t} = \tau t, \quad \hat{\Omega} = \frac{\Omega}{\tau},$$

$$\hat{J} = \frac{J}{mL^2}, \quad \alpha_v = \frac{\varepsilon A_v L^3}{2EI d_v^3}, \quad \alpha_w = \frac{\varepsilon A_w L^3}{2EI d_w^3},$$

$$M_r = \frac{M}{mL}, \quad \tau = \sqrt{\frac{EI}{mL^4}}$$

and ignoring terms containing angular velocity and its derivatives, the non-dimensional uncoupled equations of motion are acquired.

$$\hat{v}^{(4)} + \hat{v} - \hat{J}\hat{v}'' = 0 \quad (8)$$

$$\hat{w}^{(4)} + \hat{w} - \hat{J}\hat{w}'' = 0 \quad (9)$$

at x=0

$$v = w = 0 \quad (10)$$

$$v' = w' = 0 \quad (11)$$

at x=1

$$\hat{v}''' - M_r \hat{v}'' - \hat{J}\hat{v}' = -\frac{\alpha_v V_{DC}^2}{(1-v)^2} \quad (12)$$

$$\hat{w}''' - M_r \hat{w}'' - \hat{J}\hat{w}' = -\frac{\alpha_w (V_{DC} + V_{AC})^2}{(1-\hat{w})^2} \quad (13)$$

$$v'' = w'' = 0 \quad (14)$$

3. Static analysis

The analysis of the uncoupled system in the drive and sense directions is similar. Therefore, we follow the analysis only in the drive direction. The deflection is separated into static and dynamic components:

$$\hat{w}(\hat{x}, \hat{t}) = w_s(\hat{x}) + w_d(\hat{x}, \hat{t}) \quad (15)$$

Substituting equation (15) into (9), the static equation of motion is obtained:

$$w_s^{(4)} = 0 \quad (16)$$

Applying boundary conditions, the solution can be represented as follows:

$$w_s(\hat{x}) = C(-3\hat{x}^2 + \hat{x}^3) \quad (17)$$

where C is the solution of the following equation:

$$C(1+2C)^2 = -\frac{\alpha_v V_{DC}^2}{6} \quad (18)$$

4. Natural frequencies

The natural frequencies of the uncoupled system are obtained by solving the eigenvalue problem. Substituting (15) into (9)-(14) the dynamic equations of motion are determined:

$$w_d^{(4)} + \hat{w}_d - \hat{J}\hat{w}_d'' = 0 \quad (19)$$

at x=0:

$$w_d = 0, \quad w_d' = 0 \quad (20)$$

at x=1:

$$w_d''' - M_r \hat{w}_d'' - \hat{J}\hat{w}_d' = -\frac{\alpha_w V_{DC}^2}{(1-w_d)^2} \quad (21)$$

$$w_d'' = 0 \quad (22)$$

Assuming solution of the form:

$$w_d(\hat{x}, \hat{t}) = \Phi(\hat{x})e^{i\omega\hat{t}} \quad (23)$$

the eigenvalue problem is obtained:

$$\Phi^{(4)}(\hat{x}) - \omega^2\Phi(\hat{x}) + \omega^2\hat{J}\Phi''(\hat{x}) = 0 \quad (24)$$

$$\Phi(0) = 0, \quad \Phi'(0) = 0 \quad (25)$$

$$\Phi''(1) = 0 \quad (26)$$

$$\begin{aligned} &\Phi'''(1) + \omega^2 M_r \Phi(1) + \omega^2 J \Phi'(1) \\ &= -\frac{2\alpha_w V_{DC}^2 \Phi(1)}{(1-w_s(1))^3} \end{aligned} \quad (27)$$

where $w_s(1)$ is static deflection at the end of the beam. Solution of equation (24) is given by:

$$\begin{aligned} \Phi(\hat{x}) = &A_1 \sin \Lambda_1 + A_2 \cos \Lambda_1 \\ &+ A_3 \sinh \Lambda_2 + A_4 \cosh \Lambda_2 \end{aligned} \quad (28)$$

where

$$\Lambda_1 = \hat{x} \sqrt{\frac{1}{2}(\omega\sqrt{\alpha^2\omega^2 + 4} + \alpha\omega^2)} \quad (29)$$

$$\Lambda_2 = \hat{x} \sqrt{\frac{1}{2}(\omega\sqrt{\alpha^2\omega^2 + 4} - \alpha\omega^2)} \quad (30)$$

Applying boundary conditions to the general solution, and following standard procedures, a characteristic equation is

obtained and solved for ω . The static pull-in voltage is the point where ω reaches zero.

5. Numerical results

The following numerical values for the micro beam gyroscope are used to display the effect of design parameters on pull-in voltage and fundamental frequency.

Table 1. Design parameters.

Symbol	Description	Unit	Value
L	Beam length	μm	400
ρ	Density	kg / m^3	2300
E	Young's modulus	N / m^2	160×10^9
M	Tip mass	kg	7.212×10^{-12}
m	Mass per unit length	kg / m	1.8×10^{-8}
b	Beam width	m	2.8×10^{-6}
h	Beam thickness	m	2.8×10^{-6}

In order to validate the results and the applied method, a comparison is performed using the numerical results presented in the literature. In Figure 2 variation of fundamental frequency with the input DC voltage obtained from the current research is compared with those of Ghommem et al. for three values of non-dimensional mass [15]. As can be seen, the results show great agreement.

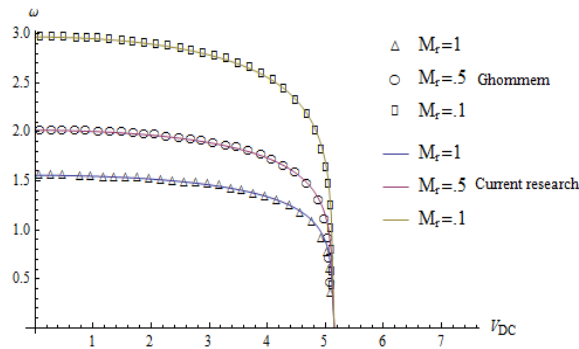


Fig. 2. Fundamental frequencies vs. input DC voltage

Figures 3 to 7 show the variation of the fundamental frequency with the DC voltage for different values of design parameters. It is evident from the results that the pull-in voltage is independent of the values of tip mass (M) and the values of the mass per unit length (m). The first natural frequency is directly

proportional to the value of mass per unit length. Meanwhile it is inversely proportional to the value of tip mass. Increasing the Young's modulus (E) or the cross-sectional second moment of area (I) results in higher pull-in voltages. However, there is no significant effect on fundamental frequency in voltages well under the pull-in voltage. Pull-in voltage tends to decrease as the beam length (L) increases, while first natural frequency slightly increases with higher beam length.

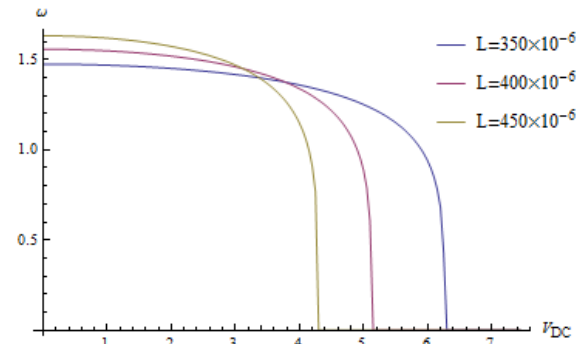


Fig. 3. Variation of the first natural frequency with DC voltage for various values of beam length

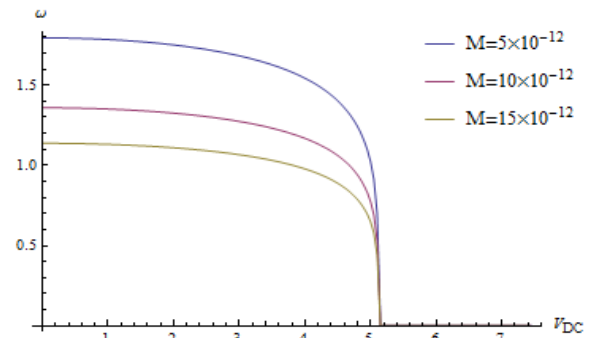


Fig. 4. Variation of the first natural frequency with the DC voltage for various values of the tip mass

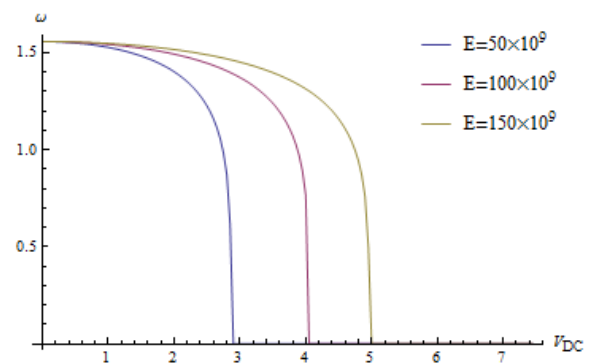


Fig. 5. Variation of the first natural frequency with DC voltage for various values of the Young's modulus

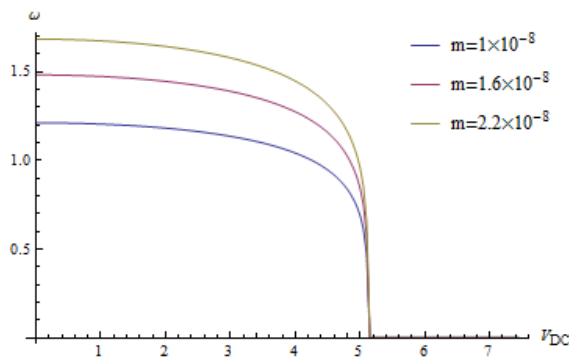


Fig. 6. Variation of the first natural frequency with DC voltage for various values of the mass per unit length

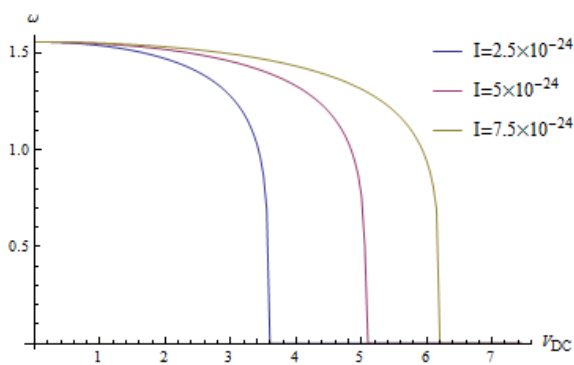


Fig. 7. Variation of the first natural frequency with DC voltage for various values of the cross-sectional second moment of area

6. Conclusions

In this study, model of a beam micro-gyroscope was used to study the effect of design parameters on pull-in voltage and natural frequency of a micro-gyroscope. The uncoupled equations of motion were derived and solved for different values of DC voltage and design parameters. The results illustrate how the pull-in voltage and natural frequency of the beam micro-gyroscope depends on design parameters and can provide researchers a guideline to satisfy the design requirements.

References

[1].Moghimi Zand M., 2012, The dynamic pull-in instability and snap-through behavior of initially curved microbeams, *Mechanics of Advanced Materials and Structures*, **19**: 485–491.

[2].Mojahedi M., Moghimi Zand M., Ahmadian M.T., Babai M., 2011, Analytic solutions to the oscillatory behavior and primary resonance of electrostatically actuated microbridges,

International Journal of Structural Stability and Dynamics, **11**(6): 1119-1137.

- [3].Moghimi Zand M., Ahmadian M.T., 2010, Dynamic pull-in instability of electrostatically actuated beams incorporating Casimir and van der Waals forces, in *Proceedings of the Institution of Mechanical Engineers, Part C, Journal of Mechanical Engineering Science* **224**(9): 2037-2047.
- [4].Moghimi Zand M., Rashidian B., Ahmadian M.T., 2010, Contact time study of electrostatically actuated microsystems, *Scientia Iranica, Transaction B: Mechanical Engineering* **17**(5): 348-357.
- [5].Mojahedi M., Moghimi Zand M., Ahmadian M.T., 2010, Static pull-in analysis of electrostatically actuated microbeams using homotopy perturbation method, *Applied Mathematical Modelling* **34**(4): 1032-1041.
- [6].Moghimi Zand M., Ahmadian M.T., Rashidian B., 2009, Semi-analytic solutions for nonlinear vibrations of microbeams under suddenly applied voltages, *Journal of Sound and Vibration* **325**(1-2): 382-396.
- [7].Moghimi Zand M., Ahmadian M.T., 2009, Application of homotopy analysis method in studying dynamic pull-in instability of microsystems, *Mechanics Research Communications* **36**(7): 851-858.
- [8].Tajalli S.A., Moghimi Zand M., Ahmadian M.T., 2009, Effect of geometric nonlinearity on dynamic pull-in behavior of coupled-domain microsystems based on classical and shear deformation plate theories, *European Journal of Mechanics - A/Solids* **28**(5): 916-925.
- [9].Moghimi Zand M., Ahmadian M.T., 2009, Vibrational analysis of electrostatically actuated microstructures considering nonlinear effects, *Communications in Nonlinear Science and Numerical Simulations* **14**(4): 1664-1678.
- [10]. Moghimi Zand M., Ahmadian M.T., 2007, Characterization of coupled-domain multi-layer microplates in pull-in, vibrations and transient behavior, *International Journal of Mechanical Sciences* **49**(11): 1226-1237.
- [11]. O'Connor J. M., Shupe D. M., 1983, Vibrating beam rotating sensor, *U.S. Patent* **4**: 381 672.
- [12]. Maenaka K., Fujita T., Konishi Y., Maeda M., 1996, Analysis of a highly sensitive silicon gyroscope with cantilever beam as vibrating

- mass, *Sensors and Actuators A: Physical* **54**(1-3), 568–573.
- [13]. Seok J., Scarton H.A, 2006, Dynamic characteristics of a beam angular-rate sensor, *International Journal of Mechanical Sciences* **48**(1): 11–20.
- [14]. Esmaeili M., Jalili N., Durali M., 2007, Dynamic modelling and performance evaluation of a vibrating beam microgyroscope under general support motion, *Journal of Sound and Vibration* **301**(1-2): 146–164.
- [15]. Ghommen M., Nayfeh A.H., Choura S., Najjar F., Abdel-Rahman E.M., 2010, Modelling and performance study of a beam microgyroscope, *Journal of Sound and Vibration* **329**: 4970–4979.